ISSN 1063-7834, Physics of the Solid State, 2016, Vol. 58, No. 8, pp. 1622–1626. © Pleiades Publishing, Ltd., 2016.
Original Russian Text © V.M. Egorov, Yu.M. Boiko, V.A. Marikhin, L.P. Myasnikova, E.I. Radovanova, 2016, published in Fizika Tverdogo Tela, 2016, Vol. 58, No. 8, pp. 1568–1572.

MECHANICAL PROPERTIES, PHYSICS OF STRENGTH, AND PLASTICITY

A Study of Ultra-Strength Polymer Fibers via Calorimetry

V. M. Egorov*, Yu. M. Boiko, V. A. Marikhin, L. P. Myasnikova, and E. I. Radovanova

Ioffe Physical-Technical Institute, Russian Academy of Sciences,
Politekhnicheskaya ul. 26, St. Petersburg, 194021 Russia
**e-mail: victor_egorov1@inbox.ru*

Received January 27, 2016

Abstract—Xerogel reactor powders and supramolecular polyethylene fibers with various degrees of hood have been studied via differential scanning calorimetry. A higher strength of laboratory fibers in comparison with industrial ones is found to be achieved due to a multistage band high-temperature hood that causes the thermodynamic parameters of supramolecular polymer structure.

DOI: 10.1134/S1063783416080114

Acquiring high-strength and high-module polymers is an extremely urgent task due to continuously increasing requirements to the mechanical properties of materials used in structural products. To solve this problem, high-strength and high-module polyethylene (PE)-based polymer fibers exhibit advantages over other materials in terms of their operation properties, primarily due to their low specific density, high chemical resistance, and biological passivity. In addition, they can serve as the fillers in composites.

At the end of the 1980s the DSM (Holland) and Honeywell (USA) corporations were authorized for industry-level output of supramolecular PE with a molecular weight of superior to 10^6 g/mol via a principally new gel technology [1]. This method allowed the physicomechanical characteristics of PE fibers to be drastically improved and the tensile strength σ_p of fibers to increase by several times (up to 3 GPa). It is worth mentioning that despite these corporations using different solvents during the gel process (decaline by DSM and mineral oil by Honeywell), the announced characteristics were identical. Moreover, no progress in the improving physicomechanical properties of the fabricated fibers was observed for the reported period. Evidently, a further considerable increase in the physicomechanical characteristics of fibers obtained via gel technology can only be due to a careful analysis of processes at each stage of the fiber production. In addition, it is also important to clarify the role of the solvent, because the molecules of decaline and mineral oil have different geometric shapes that are expected to affect the orientation hood process. The average tensile strength values of 4.7 GPa (near 6% samples had the values to 6.0 GPa) were attained under the laboratory conditions upon the orientation hood based on the elaborated structural and kinetic strengthening principles for superoriented PE gel threads at the Physicotechnical Institute (Russian Academy of Sciences, St. Petersburg) [2]. In connection with this, the data on thermophysic properties of these ultraoriented PE threads implemented at each stage of a multiple-stage gel technological process are of particular interest.

In this work, the thermophysical characteristics were studied for various samples, such as:

I—pristine nascent PE powder with an average-viscose molecular weight of $M_w = 3 \times 10^6$;

II—xerogel films (IIa—xerogel based on 1% solution in mineral oil and IIb—xerogel based on 1.5% solution in decaline);

III—xerogel films with different degree of hood (IIIa and IIIb), acquired via the multi-stage band orientation hardening at local heaters [3] from IIa and IIb xerogels, respectively; and

IV—fibers with different degree of hood, obtained via gel technology from a PE reactor powder with the same molecular weight on an experimental industrial setup at the Research Institute of Synthetic Fiber (Tver, Russia). Vaseline oil was used as the solvent.

The aforementioned samples were probed on a DSC-2 Perkin–Elmer calorimeter while varying the heating rate V from 0.3 to 5 K/min. The temperature scale was calibrated from the ice and indium melting points (273.1 K and 429.7 K, respectively), and the heat flow scale was aligned with respect to the sapphire thermal capacity, whereas the thermal effect determined from the area in a DSC curve was gauged from the indium melting enthalpy ($\Delta H_f = 6.80$ cal/g).

The thermophysical characteristics in DSC devices can be simple enough, due to the lack of visible methodical errors. In fact, they are that, if determining only the energy effects; i.e., the measuring enthalpy of the sample ΔH, because such parameters as the sam-

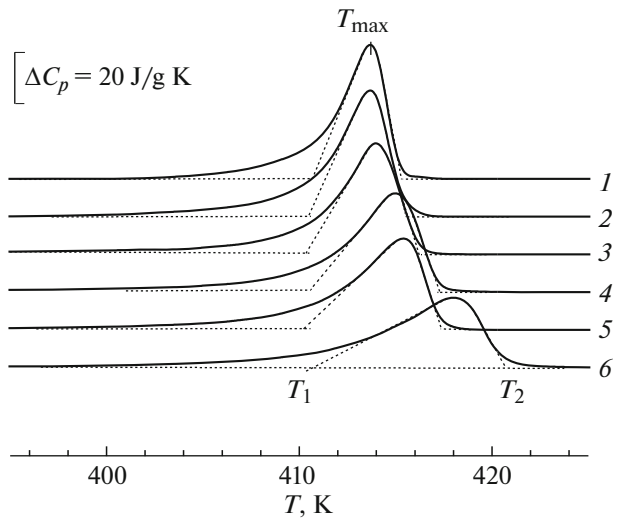

Fig. 1. The DSC curves acquired in heating with various rates of the equally weighted samples I (6 mg) V, K/min: *1*—0.31, *2*—0.62, *3*—1.25, *4*—2.5, *5*—5, and *6*—10.

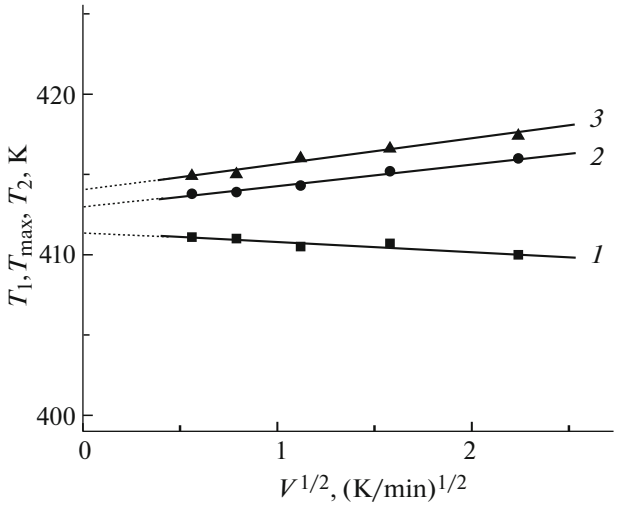

Fig. 2. Temperature parameters of the melting peak T_1 (*1*), T_{max} (*2*), and T_2 (*3*) for equally weighted samples I (6 mg) as a function of the heating rate V.

ple weight, scanning rate, and thermal contact of the sample with the capsule exerting no influence on the ΔH value. Nevertheless, some methodical difficulties can arise in determination of the true temperature parameters (T_{tr}) of heat effects. They are caused by the need to take into account and eliminate the so-called effect of thermal resistance of the sample in a capsule; i.e., inhomogeneous heating or cooling of the sample to the temperature of capsule which is detected by a device (T_{exp}). Without integrating this effect, the error in the measuring temperature characteristics from a DSC curve increases with the weight of the studied sample and with the scanning rate. If studying the nascent PE powders, the poor contact of the sample with the capsule contributes to the thermal resistance, because the reactor powders consist of the porous spherical particles and are in contact with the plane surface of the heating cell.

These methodical factors can be integrated for materials without the structural transformations upon the temperature scanning. As was shown in [4], the error in the determination of true temperatures from the DSC curves $\Delta T = T_{exp} - T_{tr}$ is proportional to the scanning rate V, sample weight m, and thermal resistance R with respect to a ratio $\Delta R \sim (m^*R^*V)^{1/2}$. At a constant R and the samples with the identical weight it is natural to expect a linear dependence of $\Delta T(V^{1/2})$. At $V \to 0$ the difference $\Delta T \to 0$ and $T_{exp} \to T_{tr}$, as well as extrapolating the dependence $\Delta T(V^{1/2})$ to a zero scanning rate, results in T_{tr}.

A considerably increased laboriousness does not allow the frequent implementation of these studies, and most of the published data, including those for nascent powders and PE fibers, must be corrected. In this work, the calorimetric study of the powder and fiber melting was implemented in heating while varying the rate from 0.3 to 5–10 K/mm. Since the melting erases all peculiarities of the pristine structure in the powder and fibers, no temperature scanning upon cooling from the melt, i.e., crystallization fixing, was conducted.

Figure 1 displays the DSC curves acquired in heating of the nascent PE powder samples with the equal weight (6 mg). Obviously, the curves obtained at the same material with varying the scanning rate are strongly different, as well as the experimental temperature characteristics of the melting peak T_1, T_{max}, and T_2. Calculated from these DSC curves, the melting enthalpy of the samples gives the constant Δ = 206 J/g value at the measuring error of 1.5% for the curve area and sample weight. The degree of crystallinity determined from the obtained melting enthalpy as $\chi = (\Delta H/\Delta H^0) \times 100\%$ (where $\Delta H^0 = 290$ J/g [5]) is $\chi = 70\%$.

The determination of the true temperature parameters of the melting point needs plotting the $T_1(V^{1/2})$, $T_{max}(V^{1/2})$, and $T_2(V^{1/2})$ dependences and extrapolating them to a zero heating rate in the case of their linearity. These dependences are shown in Fig. 2. Evidently, the experimental points for the $T_1(V^{1/2})$, $T_{max}(V^{1/2})$, and $T_2(V^{1/2})$ match the straights *1–3*, and their extrapolation to a zero heating rate results in the true T_1, T_{max}, and T_2 temperatures, whose values are given in the table. We note that the straight slope is determined by the sample weight and the R parameter, which were fixed as constant in our measurements. The DSC data were used to estimate one more characteristic of the supramolecular polymer structure, which is the intrachain melting cooperativity (ν). Its physical meaning is to determine a minimum

Thermodynamic parameter of the melting peak for the studied samples

Number of sample	λ	T_1, K	T_{max}, K	T_2, K	ΔT, K	ν	L, nm	ΔH, J/g	χ, %
I	–	411.6	412.6	413.6	2.0	175	21	206	70
IIa	–	405.6	407.5	408.4	2.8	120	15	219	75
IIb	–	407.0	408.2	408.9	1.9	180	22	218	75
IIIa	9	412.3	412.7	413.0	0.7	500	62	202	69
IIIa	45	415.0	415.2	415.3	0.3	1170	145	205	70
IIIa	95	415.55	415.55	415.45	0.1	3500	435	256	87
IIIa	170	415.25	415.20	415.17	0.08	4400	540	262	90
IIIb	13	412.9	413.2	413.5	0.6	580	72	220	76
IIIb	45	413.9	414.1	414.3	0.4	870	108	220	76
IIIb	100	415.05	415.1	415.15	0.1	3500	435	255	87
IV	32	416.1	416.5	416.9	0.8	442	55	220	76
IV	41	415.8	416.5	417	1.2	295	36	228	78
IV	82	415.9	416.3	417	1.1	320	40	224	77
IV	84	416.2	416.5	417	0.8	440	55	254	87

sequence of the ν parameters of the repeating units in the chain, which pass as a whole of the crystallite into a folded state of a statistical coil in the melt [6, 7]. The ν parameter was estimated using a formula:

$$\nu = 2\mathcal{R}(T_{max})^2/\Delta T\Delta H^0,$$

where $\mathcal{R}$ is the gas constant. The dimensionless ν parameter is expressed by a number of the CH_2 groups in the transsegment of the PE chain, which participate simultaneously in the melting. If multiplying ν by a length of the C–C unit bond (the size of the C–C bond projection of the main chain onto the macromolecule axis $h = 0.124$ nm), this parameter $L = \nu h$ can be compared with the supramolecular structure ones, including the lamellar formation dimensions [8]. For the reactor powder samples, the L magnitude evaluated from the cooperativity parameter ν equals 21 nm and is comparative with the lamellar crystal thickness.

The identical DSC curves were acquired for the xerogel samples prepared using mineral oil (IIa) and decaline (IIb). The true temperature parameters of the melting point were also determined from the curves, the $T_1(V^{1/2})$, $T_{max}(V^{1/2})$, and $T_2(V^{1/2})$ dependences, and their extrapolation to a zero heating rate enabled us to obtain their true T_1, T_{max}, and T_2 temperatures. The true T_1, T_{max}, and T_2 temperatures, the melting enthalpy ΔH, the degree of crystallinity χ, and the lamellar crystal thickness evaluated from the ν cooperativity parameters for IIa and IIb xerogel samples are shown in the table.

A comparison of the data in the table for the nascent powder and xerogels reveals an apparent contradiction: the melting point in the nascent powder is higher, while the degree of crystallinity is lower than in xerogels. This can be explained by different supramolecular structure. In the reactor powder the significant portion of the bulk is occupied by the fibrillary formations, whereas the lamellar ones are predominant in xerogels. The fibrillary r structures hamper the melting of lamels because of a relatively high amount of the communicating molecules, which couple the lamels between each other and impede their transition into the disordered state in melting. As is shown in the model experiments [9] on extremely oriented PE fibers, this obstacle favors an increase in the melting point. The different crystallinity is due to various conditions of the supramolecular structure formation. During the powder synthesis in the reactor the conditions of the structure formation are nonequilibrium rather than in the preparation of xerogel. As follows from the comparative estimation of the thermophysical parameters of xerogels from decaline and mineral oil, the first are more perfect. Despite the fact that they possess the same degree of crystallinity (75%), the melting point of the decaline-based xerogel is higher, the melting cooperativity parameter is superior, and the melting peak width is smaller than in the xerogel made with mineral oil.

The DSC study of the thermodynamic characteristics of fibers and film threads has additional methodical difficulties. In particular, using the bulk samples with a weight of 1–5 mg (the length of one fiber is ~1 m) causes an abrupt increase in the thermal resistance R and the rising error ΔT upon the sample styling in the capsule. Even using the short fiber segments (~5 mm) as the samples results in the scattering temperature parameters of the melting peak from sample to sample (Fig. 3), which testifies to the variability of R at the same sample weight. An additional thermoconductive medium between the sample and the cap-

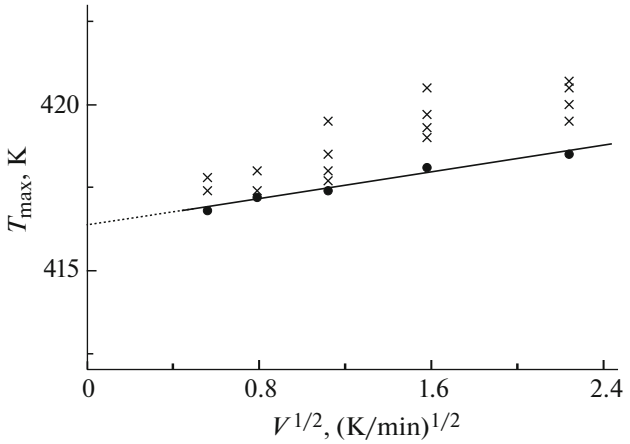

Fig. 3. T_{max} parameter of the melting peak as a function of heating rate for samples IV ($\lambda = 82$) with the weight of ~0.05 mg in a thermoconductive medium (the Wood's alloy) and without a thermoconductive environment (denoted with the crosses).

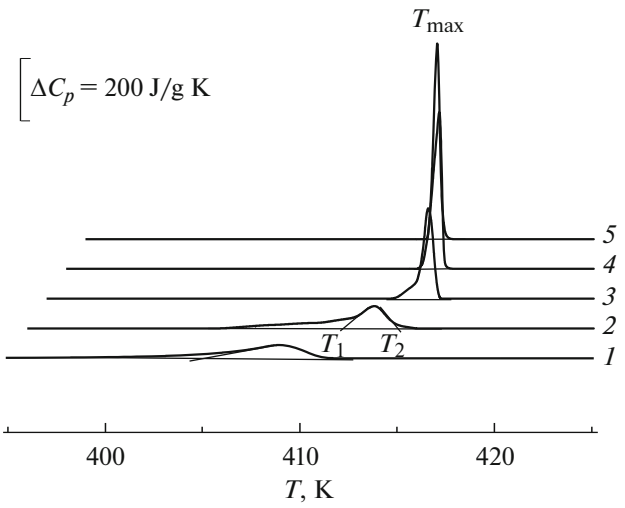

Fig. 4. The DSC curves acquired in heating ($V = 5$ K/min) of samples IIa (*1*) and IIIb (*2–5*). The hood is $\lambda = 9$ (*2*) 43 (*3*), 95 (*4*), and 170 (*5*).

sule allows the thermal resistance to be considerably decreased and stabilized. For this, the Wood alloys with a tunable melting point inferior to that of fiber were used. When putting the ~5 mm fiber segment into the Wood alloy foil, both are subsequently molten upon heating so that the sample is inside the metal liquid with the high thermal conductivity. As is seen from Fig. 3, the melting point of fiber in this case is found to be minimum at all used heating rates, and the experimental points for the $T_{max}(V^{1/2})$ relation fit well the linear dependence. This technique was further used in studying the fibers.

Figure 4 shows the DSC curves of one of the studied samples with the changing thermodynamic parameters of the melting peak with the hood. Here, the T_1, T_{max}, and T_2 temperatures increase, whereas the peak shape exhibits transformations. Its amplitude rises with the emergence of a low-temperature wing at the first stage ($\lambda < 50$) due to the defrosting mobility in the communicating straightened parts of molecules, which connect the crystallites between each other. This wing vanishes at high degrees of hood that is caused by the transition of these parts in molecules from amorphous to crystal state. The quantitative characteristics of the changing thermodynamic parameters of the melting peak were revealed in the experiments on the determination of the $T_1(V^{1/2})$, $T_{max}(V^{1/2})$, and $T_2(V^{1/2})$ dependences and their extrapolation to a zero heating rate. The true temperature parameters of the melting peak, the temperature melting and melting enthalpy ranges, as well as the calculated intrachain cooperative melting parameter ν and the crystal thickness L, are shown in the table.

It is obvious from the data in the table that the most conservative parameter is the melting temperature T_{max} which increases in the limits of 1–2.5 K with the degree of hood. The melting enthalpy ΔH and the degree of crystallinity χ are more sensitive to the changing λ, which increase by 10–30% at high degrees of hood. It is worth mentioning that starting with the comparatively low hood from the neck ($\lambda = 9$–10) to $\lambda = 45$, these parameters drop in comparison with the data for xerogel. The most pronounced changes are observed in the temperature melting range of ΔT_f and its related parameters ν and L. It is seen in the table that the intrachain cooperative melting parameter ν and L increase by dozens of times with the rising hood. At $\lambda = 170$ the cooperative domain size in the xerogel-based fiber in the transition from the crystal to liquid state attains ~0.5 μm.

If referring to Fig. 5, an increase in L for these samples passes evidently in two stages. At the first one, a neck is formed and the polymer structure is intermediate from lamellar to fibrillary. The last one is characterized by a high amount of the straightened connecting sites of molecules that couple the crystallites in microfibrilles. From the dynamical point of view these segments of molecules are liquid, and no additional contribution to the melting enthalpy of the whole sample is thus expected. At the second stage ($\lambda > 50$), the above molecule segments pass the liquid-to-crystal state transformation that favors an increase in the melting enthalpy of the whole sample. It is important to note that the second stage is missing in the industrial samples, and the L parameter remains unchanged over the range of $L = 30$–85. At the same time, for the xerogel film-based fibers, the L parameter rises at the second stage with λ being independent on the type of solvent.

If considering the direct relationship of the ν and L parameters with the strength characteristics of polyethylene [10], one can expect a pronounced increase

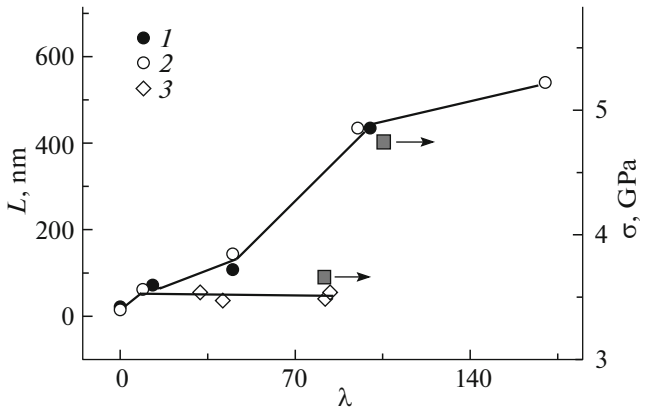

Fig. 5. Correlation parameter L as a function of the hood of samples IIIb (*1*), IIIa (*2*) and IV (*3*). The tensile strength of samples IIIa, IIIb and IV are marked with the arrows.

in the strength at the second stage ($\lambda > 50$) for fibers obtained from the xerogel film.

The mechanical tests indeed revealed that the tensile strength σ_t at $\lambda = 90–120$ for the samples IIIa and IIIb attains the values of 4.0–5.8 GPa (the mean σ_t values of the samples prepared from decaline and mineral oil are equal, being 4.7 GPa). At the same time, the strength of the industrial fibers IV enriches the values of 3.7–3.9 GPa. This circumstance testifies to the potentiality of increasing the mechanical properties of the industrial fibers acquired via gel technology, because the mechanical characteristics of film threads obtained via extension of xerogels under the laboratory conditions were found to be much higher than those of the industrially prepared gel-oriented fibers.

The above data enable us to conclude that solving the problem of a noticeable increase in the mechanical characteristics of the industrial product is in a careful establishment of the temperature and force orientation modes at the second stage ($\lambda > 50$), at which the cooperative melting domain sizes L will symbatically increase with using the multistage band high-temperature hood.

ACKNOWLEDGMENTS

We are grateful to a staff of the Research Institute of Synthetic Fiber "VNIISV" (Tver, Russia) for providing the samples for this work.

REFERENCES

1. P. Smith and P. J. Lemstra, J. Mater. Sci. **15**, 505 (1980).
2. V. A. Marikhin and L. P. Myasnikova, Prog. Colloid Polym. Sci. **92**, 39 (1993).
3. V. A. Marikhin and L. P. Myasnikova, Macromol. Chem., Macromol. Symp. **41**, 209 (1991).
4. K. Illers, Eur. Polym. J. **10**, 911 (1974).
5. B. Wunderlich, *Macromolecular Physics*, Vol. 3: *Melting of Polymers* (Academic, New York, 1980; Mir, Moscow, 1984), p. 64.
6. P. Flory, J. Polym. Sci., Part B **49**, 105 (1961).
7. S. Ya. Frenkel', *Encyclopedia of Polymers* (Sovetskaya Entsiklopediya, Moscow, 1974), Vol. 2, p. 100 [in Russian].
8. V. A. Berstein, A. V. Savitskii, V. M. Egorov, I. A. Gorshkova, and V. P. Demicheva, Polym. Bull. (Heidelberg, Ger.) 12, 165 (1984).
9. V. A. Berstein, V. M. Egorov, V. A. Marikhin, and L. P. Myasnikova, Int. J. Polym. Mater. **22**, 167 (1993).
10. V. A. Bershtein, V. M. Egorov, V. A. Marikhin, and L. P. Myasnikova, Vysokomol. Soedin., Ser. A **32**, 2380 (1990).

Translated by O. Maslova